JACS
JOURNAL OF THE AMERICAN CHEMICAL SOCIETY
Article
pubs.acs.org/JACS

Mechanism and Stereoselectivity of a Dual Amino-Catalyzed Robinson Annulation: Rare Duumvirate Stereocontrol

Matthew D. Pierce, Ryne C. Johnston, Subham Mahapatra, Hua Yang, Rich G. Carter, and Paul Ha-Yeon Cheong*

Department of Chemistry, Oregon State University, 153 Gilbert Hall, Corvallis, Oregon 97331, United States

Supporting Information

ABSTRACT: Computational study of the mechanisms and stereoselectivities of a dual amino-catalyzed synthesis of cyclohexenones containing all-carbon γ-quaternary and ∂-tertiary stereocenters is reported. Extensive conformational search with density functional theory optimizations, the high-accuracy SCS-MP2/cc-pV∞Z energies, and PCM solvation corrections were used to characterize all intermediates and transition states. Six mechanisms were considered, all consistent with available experiments. The reaction proceeds via sequential Michael and Mannich conjugate additions whereby the primary amine activates the aldehyde and the catalyst activates the pentenone. We have discovered a rare duumvirate stereocontrol: the Michael reaction sets the enantioselectivity, but both the Michael and the Mannich reactions control the diastereoselectivity.

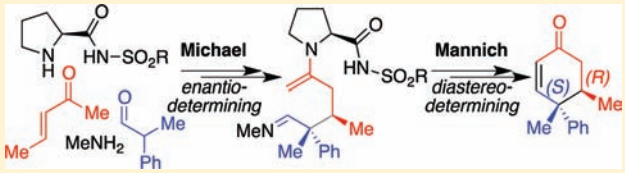

1. INTRODUCTION

The development of atom-[1] and step-economical[2] catalytic methods to access all-carbon quaternary stereocenters is an important goal in organic synthesis.[3] Toward this end, the Carter group (H.Y., R.G.C.) recently reported a one-pot, highly enantio- and diastereoselective organocatalytic methodology for the synthesis of cyclohexenones **5** containing γ-quaternary and ∂-tertiary all-carbon stereocenters catalyzed by proline sulfonamides **1** and a primary amine additive **2** (Scheme 1).[4]

Scheme 1

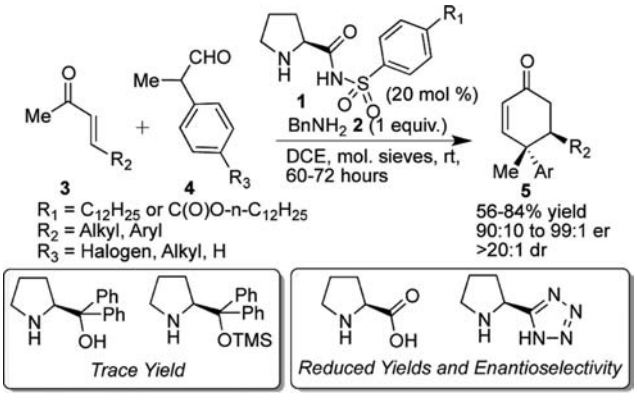

We (M.D.P., S.M., P.H.Y.C.) have conducted a detailed computational study of this reaction: an extensive conformational search with DFT (B3LYP[5]/6-31G*[6] and M06[7]), PCM solvation corrections,[8] and energy refinements at the basis set limit[9] of SCS-MP2.[10] For the six mechanisms studied, we found that the reaction proceeds via a Michael/Mannich cascade. Remarkably, this reaction manifests a duumvirate stereocontrol: the first Michael step controls the enantioselectivity, while both the Michael and the Mannich reactions control the diastereoselectivity.

The reaction is a formal Robinson annulation[11] between alkyl,aryl α,α-disubstituted aldehydes **4** and β-substituted enones **3** (Scheme 1). No reaction is observed in the absence of a primary amine or the proline sulfonamide catalyst **1**. Although technically catalytic, stoichiometric amounts of primary amine **2** are necessary for reasonable rates of reaction. Use of molecular sieves resulted in a significant increase in stereoselectivity. This is in contrast to similar reactions where water is tolerated or even beneficial.[12] The electron-deficient version of the sulfonamide catalyst (R_3=C(O)O-n-$C_{12}H_{25}$) exhibits a slightly improved enantioselectivity with most substrates. A relatively acidic hydrogen bond donor is required for reactivity, as prolinol derivatives gave trace yield. Proline and the tetrazole gave significantly reduced yields and enantioselectivities. Simple carboxylic acids and sterically hindered amines, e.g. α-methyl benzylamine, do not catalyze the reaction.

2. METHODS

To realize optimal computational efficiency while retaining chemical relevance, the aryl group of sulfonamide **1** and the benzyl of amine additive **2** were modeled as methyl. Allylamine has been successfully used in this reaction with minimal changes in yield or stereoselectivity,[13a] suggesting that steric bulk at the β position on the primary amine component is not critical to the stereoselectivity or the mechanism. Also, methyl proline sulfonamides have been shown to have pK_a's nearly identical to those of the aryl-substituted

Received: February 27, 2012
Published: April 28, 2012

   dx.doi.org/10.1021/ja3018219 | J. Am. Chem. Soc. 2012, 134, 13624–13631

sulfonamides, minimizing the electronic influence of the aryl substituent on the catalyst side-chain acidity (~9.5 in DMSO).[14]

Considerable efforts were expended to capture all relevant conformations of transition states and intermediates as well as refine the relative energetics. Manual, exhaustive conformational searches were performed for all key carbon−carbon bond-forming transition structures and intermediates. For each stereoisomer, ~30 structures within 10 kcal/mol were located. Geometries and thermodynamic corrections were computed at the B3LYP[5]/6-31G* [6] level of theory.[15] The energies were refined with Grimme's spin component scaled MP2 (SCS-MP2)[10] method, extrapolated to infinite basis set[9] from the Dunning cc-pVTZ and cc-pVQZ energies (hereafter called SCS-MP2/∞). Single-point solvation corrections for dichloroethane (DCE) were performed using PCM with the UAKS radii at the B3LYP/6-31+G(d,p) level of theory.[8] Key transition states and several intermediates were also optimized with M06/6-31G*.[16] The above combination of methods (SCS-MP2/∞//B3LYP/6-31G*) was key to this study; it enabled us to accurately assess the relative stabilities of a chemically diverse range of C−C bond-forming transition states.

Accurately computing the barriers and reaction exothermicities of widely different types of mechanisms is known to be challenging for many methods.[17] In this particular system, both B3LYP and M06 were found to be problematic.

B3LYP energies were particularly problematic—B3LYP predicts artificially large instabilities for virtually every intermediate and transition state on the reaction coordinate—greater than ~20 kcal/mol higher than SCS-MP2 corrected values.[17] Not only are the individual barriers artificially high, it also incorrectly predicts that the overall reaction is endergonic by 9.3 kcal/mol. Interestingly, the relative energies between different transition-state conformations for a given C−C bond-forming step are the same with B3LYP and SCS-MP2 energies. SCS-MP2/∞ energy refinements to the B3LYP structures and thermodynamic corrections were necessary for correct predictions of stereoselectivity, reaction energetics, and comparison of barriers between steps. These errors are most likely due to the large number of van der Waals contacts present in these structures, and the success of SCS-MP2 energy corrections stems from being able to capture the energy of these interactions from B3LYP structures.

After our study was complete, M06 became available to us, and we studied the key transition structures and some intermediates with M06/6-31G* optimizations and energies. Ultimately, we continued with SCS-MP2 in the study of this particular reaction for the following reasons: (a) M06/6-31G* incorrectly predicts that the catalytic resting-state imine formation (see Figure 2) is endergonic by over 5 kcal/mol.[13b] Not surprisingly, B3LYP/6-31G* also makes this erroneous prediction. SCS-MP2/∞//B3LYP/6-31G* results are consistent with experiments in that imine formation is favored by >3 kcal/mol. (b) In the gas phase (conditions similar to the experimental toluene conditions), M06/6-31G* predicts that the Michael and Mannich steps leading to the (*R*,*R*)-diastereomer have essentially identical barriers, i.e. duumvirate selectivity is operational, consistent with SCS-MP2/∞//B3LYP/6-31G* results. When solvation corrections for DCE were included, however, M06/6-31G* predicted that the Michael addition is rate limiting for all stereoisomers. Experimentally, the reaction has been shown to give nearly identical results when significantly more nonpolar solvents, such as toluene, are employed instead of DCE.[4a] Thus a method that makes similar mechanistic predictions regardless of the inclusion of solvation corrections, such as SCS-MP2/∞//B3LYP/6-31G*, is circumstantially more likely to accurately describe this system.[16]

3. RESULTS AND DISCUSSION

Determination of the Mechanism. There are no less than six mechanisms that can account for the formation of the product (**A**−**F** in Figure 1). All levels of theory studied lead to the same mechanistic conclusion. The computed free energies of activation reveal that mechanism **A**, a Michael addition between the catalyst pentenone iminium **A1** and the aldenamine **A2** of the primary amine and the aldehyde, is operative in this transformation. Tautomerization followed by a Mannich annulation results in the formation of the observed products. The extensive hydrogen-bonding network between the approaching aldenamine and the catalyst sulfonamide oxygens

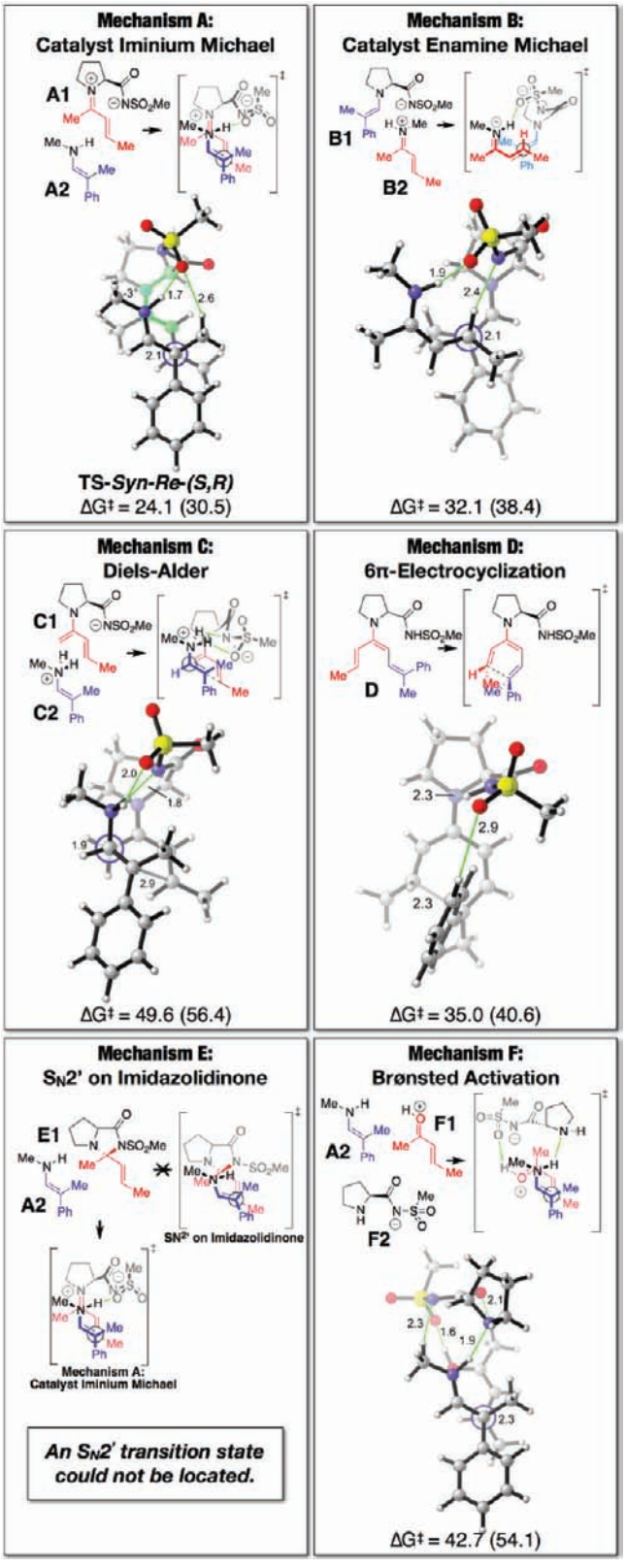

Figure 1. Rate-limiting transition structures for mechanisms **A**−**F**. Mechanism **A** is energetically favored and operative in this reaction.[21]

dx.doi.org/10.1021/ja3018219 | J. Am. Chem. Soc. 2012, 134, 13624−13631

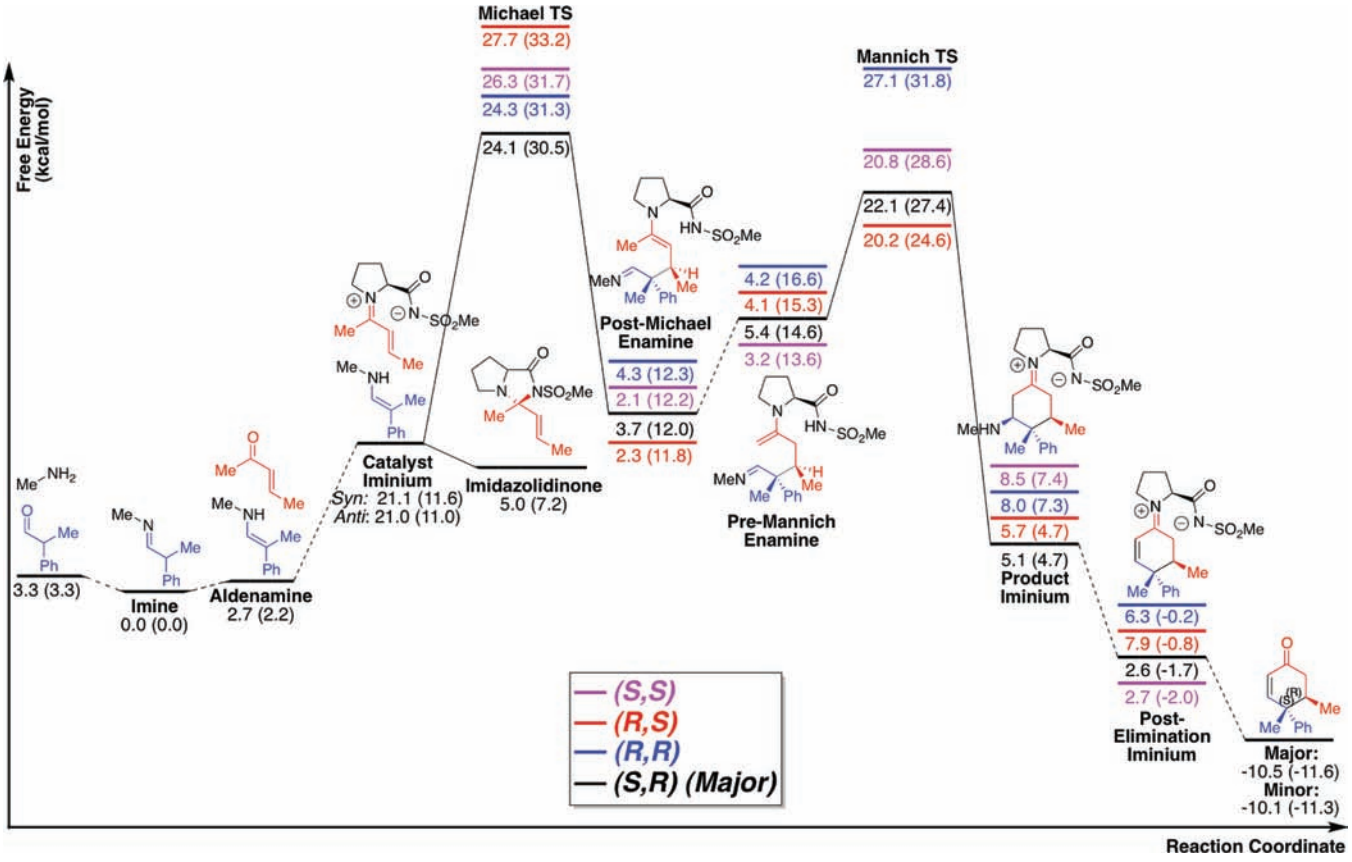

Figure 2. Reaction coordinate diagram of the operative mechanism **A**.[21]

in lieu of the amide nitrogen is significant—this explains why proline and related tetrazole are poor catalysts for this transformation.

The overall catalytic cycle is shown in Figure 2. The free energy barrier for the Michael reaction is 30.5 kcal/mol, in reasonable agreement with experimentally observed reaction rates (**TS-*Syn-Re*-(*S,R*)**, Figure 1).[18] The resting state on the reaction coordinate is the imine formed from the primary amine and the aldehyde, which is exergonic by 3.3 kcal/mol. Experimentally, premixture of the 2-phenylpropanal and benzylamine shows complete conversion to the corresponding imine by ^{1}H NMR.[13b] The imine is in a dynamic equilibrium with the nucleophilic aldenamine **A2** (ΔG = 2.2 kcal/mol), which is also favored thermodynamically relative to the starting materials. Formation of the electrophilic iminium is uphill from the imine by ∼12 kcal/mol. The Michael addition initially yields the post-Michael enamine, which tautomerizes to the reactive pre-Mannich enamine. Following Mannich cyclization, a stepwise E1cB-type elimination of the product iminium yields the thermodynamically favored and conjugated post-elimination iminium. Hydrolysis releases the product and regenerates the catalyst. The overall reaction is exergonic by ∼11.5 kcal/mol.

Mechanism **B** is the catalytic variant[19] of the Yamada−Otani reaction discovered in 1969 (Figure 1).[20] The Michael addition of mechanism **B** is higher in energy by ∼8 kcal/mol compared to mechanism **A**. This instability is presumably due to (a) the unavoidable allylic strain in the catalyst aldehyde enamine **B1** and (b) the substantial torsional strain around the forming bond.

Experimental evidence is also inconsistent with both steps of mechanism **B**. Premixture of the primary amine and aldehyde prior to the addition of catalyst and enone is required for optimum reaction rate and yield.[13a] This observation is in conflict with the expected reactive species required for the Michael addition in mechanism **B**. In addition, the regioselectivity of the amine in the subsequent Mannich annulation in mechanism **B** is inconsistent with the product regioselectivity observed in closely related reactions.[22] Specifically, in substrates where elimination is precluded due to stereoelectronic constraints, the primary amine additive is incorporated into the product (Scheme 2). If the Mannich annulation from mechanism **B** occurred, one would instead expect the chiral catalyst to be incorporated into the product.

It is also possible to account for the formation of the product via a Diels−Alder reaction (mechanism **C**, Figure 1). Both γ and β functionalizations of α,β-unsaturated carbonyl compounds using chiral secondary amines are thought to occur via a Diels−Alder mechanism, with the amine catalyzing formation of both the diene and dienophile depending on the substrates.[23] In this particular case, the Diels−Alder substrates, the catalyst pentenone dienamine and benzyl amine aldehyde enamine, are both electron rich and unlikely to undergo the Diels−Alder reaction due to electrostatic repulsion. However, proton transfer from the sulfonamide furnishes an enammonium, thus resulting in electronically matched, normal electron demand Diels−Alder intermediates. The barrier for this highly asynchronous concerted Diels−Alder process (with forming C−C bond distances of 1.9 and 2.9 Å) is 56.4 kcal/mol, more than 25 kcal/mol more disfavored than mechanism **A**. The σ-

dx.doi.org/10.1021/ja3018219 | J. Am. Chem. Soc. 2012, 134, 13624−13631

Scheme 2[22]

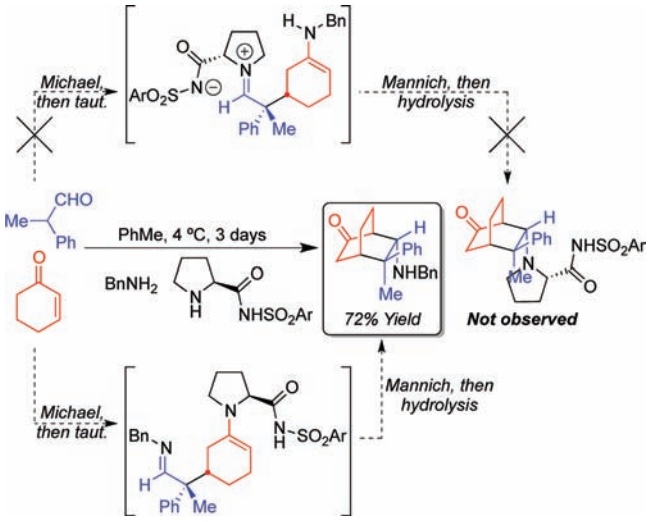

electron-withdrawing ability of the ammonium is clearly not sufficient to electrophilically activate the enammonium.

An alternative pericyclic pathway consistent with the products is 6π-electrocyclization (mechanism **D**, Figure 1). The free energy barrier for this process is 40.6 kcal/mol, more than 10 kcal/mol higher than for mechanism **A**. Consistent with our findings, high-accuracy calculations by other groups have shown that monosubstitution at the 3 position of a triene by an amine results in negligible rate enhancement.[24] In addition, the remoteness of the catalyst sulfonamide side chain from the forming C−C bond in this transition state precludes stereocontrol, also rendering this mechanism unlikely.[25] Thus, this mechanism does not display the level of reactivity or stereocontrol that is observed in the reaction.

Oxazolidinone-like intermediates, such as imidazolidinone **E1**, have been proposed as key reactive intermediates in various organocatalytic reactions (mechanism **E**, Figure 1).[26] The stability of the imidazolidinone relative to the catalyst iminium[27] (ΔG = 7.2, Figure 2) suggests that these are viable intermediates. In this context, the reaction involves an S_N2' nucleophilic attack on the catalyst pentenone imidazolidinone **E1** by the aldenamine **A2**, with the catalyst side-chain acting as an internal leaving group. All our attempts to locate such a transition structure lead to the Michael transition structure of mechanism **A**.

A final mechanistic possibility is the case where the proline sulfonamide facilitates the Michael reaction via purely intermolecular, non-covalent hydrogen-bonding interactions to both substrates (Brønsted activation, mechanism **F**, Figure 1). In this mechanism, the sulfonamide catalyst electrophilically activates the enone via protonation to form an oxocarbenium **F1** and increase the nucleophilicity of the aldenamine **A2** via general base catalysis. This transition state is found to be over 20 kcal/mol higher in energy than mechanism **A**, presumably due to the entropic cost of a trimolecular reaction.

Origins of Stereoselectivity. With the correct mechanism at hand (Figures 1 and 2), we investigated the stereoselectivity (Figures 3 and 4). The computed selectivity at SCS-MP2/∞//B3LYP/6-31G* with DCE solvation corrections ($\Delta G_{enantio}$ = 2.7 kcal/mol, $\Delta G_{diastereo}$ = 1.2 kcal/mol) agrees well with the experimental selectivity ($\Delta G_{enantio}$ = 1.3 kcal/mol, $\Delta G_{diastereo}$ = 2.0 kcal/mol) obtained using allylamine as the cocatalyst. Duumvirate control of stereoselectivity was discovered in this reaction: the Michael addition controls the enantioselectivity, while the diastereoselectivity is controlled by a combination of both the Michael and the following Mannich reaction. The Michael addition is rate-limiting for the minor (*S,S*)-product, but the Mannich annulation is the rate-determining step for the minor (*R,R*)-diastereomer (Figure 2).

Michael Addition. The lowest energy transition structures for the Michael addition are shown at the top of Figure 3. In the Michael addition, the major product arises from **TS-*Syn-Re*-(*S,R*)**, while the minor diastereomer arises from **TS-*Syn-Si*-(*R,R*)** ($\Delta G_{diastereo}$ = 0.8 kcal/mol), and the minor enantiomer from **TS-*Anti-Si*-(*R,S*)** ($\Delta G_{enantio}$ = 2.7 kcal/mol).

The stereoselectivity in the Michael step is governed by the *syn*:*anti* catalyst iminium preference and the *re*:*si* facial selectivity of the aldenamine nucleophile.

The enantiocontrol in the Michael step and the entire reaction is decided by the *anti*:*syn* catalyst iminium preference in the Michael transition states. Specifically, the *syn*-iminium transition state **TS-*Syn-Re*-(*S,R*)** leads to the major enantiomer, while the *anti* transition state **TS-*Anti-Si*-(*R,S*)** leads to the minor enantiomer. A general *syn*-iminium preference was observed in the Michael transition states, and this is the origin of enantiocontrol in this reaction.[28,29]

Interestingly, this *anti*:*syn* iminium selectivity is not the result of inherent differences in the stability of *syn* and *anti* configurations of the catalyst iminium intermediate. The lowest energy conformation of the *anti*-iminium (Figure 3, bottom left) is actually slightly favored by 0.6 kcal/mol compared to the *syn*-iminium. This disparity between ground-state and transition-state preference is in contrast to the situation found in Michael additions catalyzed by bulky diarylprolinol silyl ether type catalysts.[30] In these cases, steric factors dictate the reactive iminium by influencing ground-state stability, and the same trends of stabilities are also observed in the corresponding Michael transition states.

This *syn* preference is unusual in H-bonding-directed organocatalysts.[28,29] In the absence of other intervening effects, *syn* transition states in organocatalytic reactions are typically disfavored because the catalyst iminium/enamine must distort from planarity to accommodate the close proximity of the approaching substrate to the hydrogen-bonding catalyst side chain. In this particular reaction, the vinylogous electrophilic iminium activation in the Michael process further removes the C−C bond-forming center from the catalyst side chain, changing the optimal hydrogen-bonding distance. Specifically, the geometric distortions in the catalyst iminium necessitated by hydrogen-bonding to a more distal aldenamine consistently destabilize the *anti*-iminium Michael transition states. Thus, the *anti*-iminium transition state **TS-*Anti-Si*-(*R,S*)** features significant distortions of the planar catalyst iminium (20°, dihedral highlighted in green) compared to the **TS-*Syn-Re*-(*S,R*)** (3°, dihedral highlighted in green) and is consequently higher in energy by 2.7 kcal/mol.

The diastereocontrol in the Michael reaction is governed by the *re*:*si* aldenamine facial selectivity. The *re* transition state **TS-*Syn-Re*-(*S,R*)** leads to the major diastereomer, while the *si* transition state **TS-*Syn-Si*-(*R,R*)** leads to the minor. The *re* or *si* facial selectivity of the aldenamine in the Michael reaction is inherently poorly controlled. Calculations on a simplified model system where the chiral sulfonamide catalyst is replaced with pyrrolidine (Figure 3, bottom right) show negligible differences between the gauche interactions in the two faces of aldenamine attack (ΔG = 0.5 kcal/mol).[31] Considering the

dx.doi.org/10.1021/ja3018219 | J. Am. Chem. Soc. 2012, 134, 13624−13631

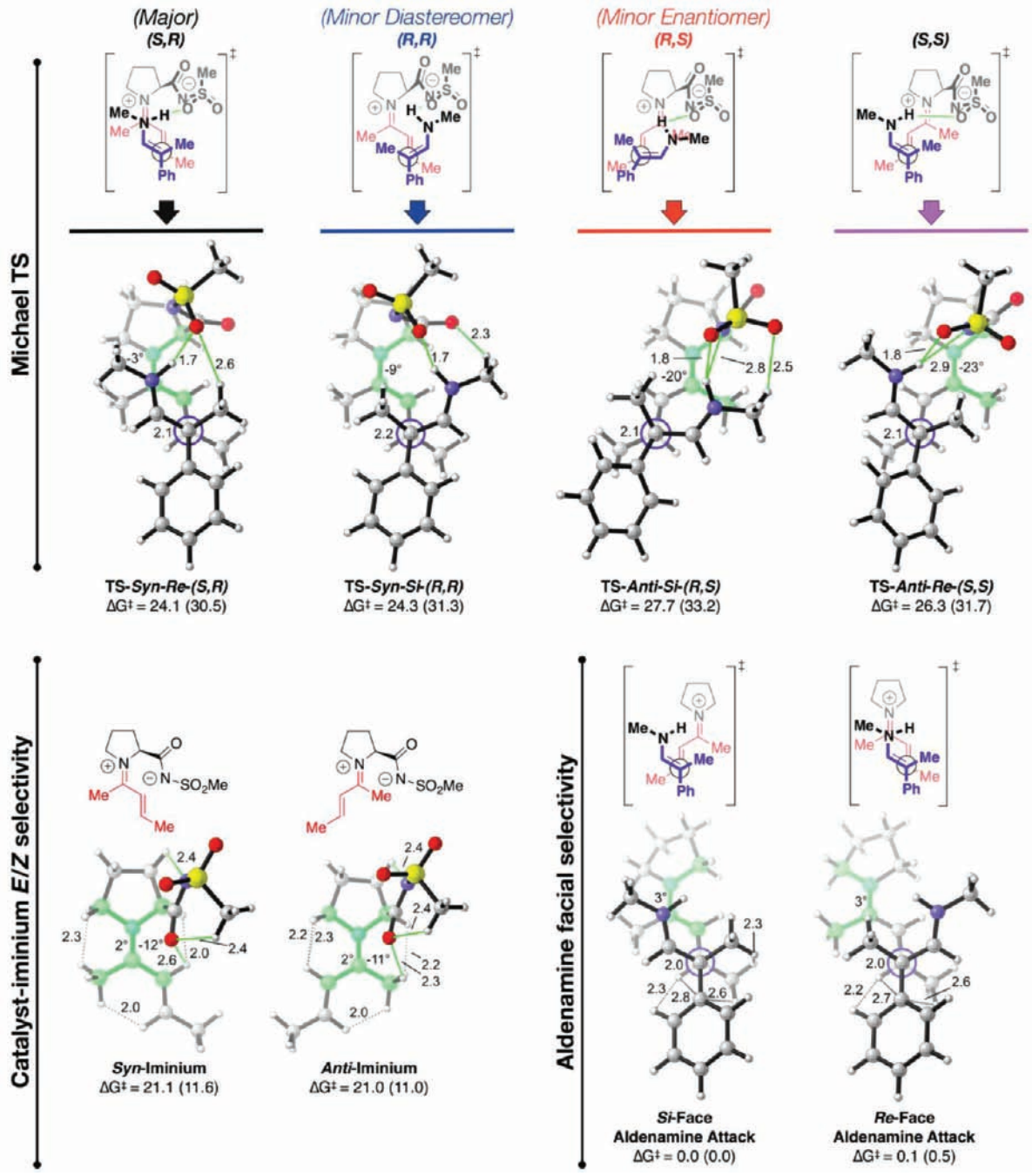

Figure 3. Above: The four Michael addition transition structures consistent with mechanism **A**, leading to the four diastereomeric cyclohexenone products. *Syn* transition structures are found to be more stable than *anti* due to greater distortions involving the iminium atoms (highlighted in green, magnitude indicated in dihedral angles). Below, left: Lowest energy conformations of the *syn* and *anti* catalyst iminiums involved in the Michael transition states. No significant energetic preference is found for either *syn* or *anti* configurations of the catalyst iminium, in contrast to the Michael transition states, where there is a strong preference for *syn* transition states. Below, right: Michael addition transition structures catalyzed by pyrrolidine. No significant energetic preference is found for either the *re* or *si* attack of the aldenamine. This is the main cause for the poor diastereoselectivity in the Michael step.[21]

preference for the major **TS-*Syn*-*Re*(*S*,*R*)** is merely 0.8 kcal/mol, this shows that the chiral hydrogen-bonding side chain contributes only ~0.3 kcal/mol of diastereocontrol.

Mannich Annulation. The lowest energy transition structures for the Mannich annulation can be seen in Figure 4. *Anti* and *syn* designations refer to the Mannich annulations where the enamine is in an *anti* or *syn* arrangement with respect to the sulfonamide side chain, respectively. The chair or boat refers to the cyclic conformation of the forming six-membered ring.

The diastereoselectivity in the Mannich annulation step and the entire reaction is decided by the stability of the Mannich annulation **TS-Boat-*Syn*-(*R*,*R*)**. The Mannich annulation transition structures leading to the other stereoisomers are lower in energy than the respective preceding Michael steps and are thus inconsequential to the stereoselectivity. **TS-Boat-*Syn*-(*R*,*R*)** has a higher barrier than any of the other Mannich

dx.doi.org/10.1021/ja3018219 | J. Am. Chem. Soc. 2012, 134, 13624–13631

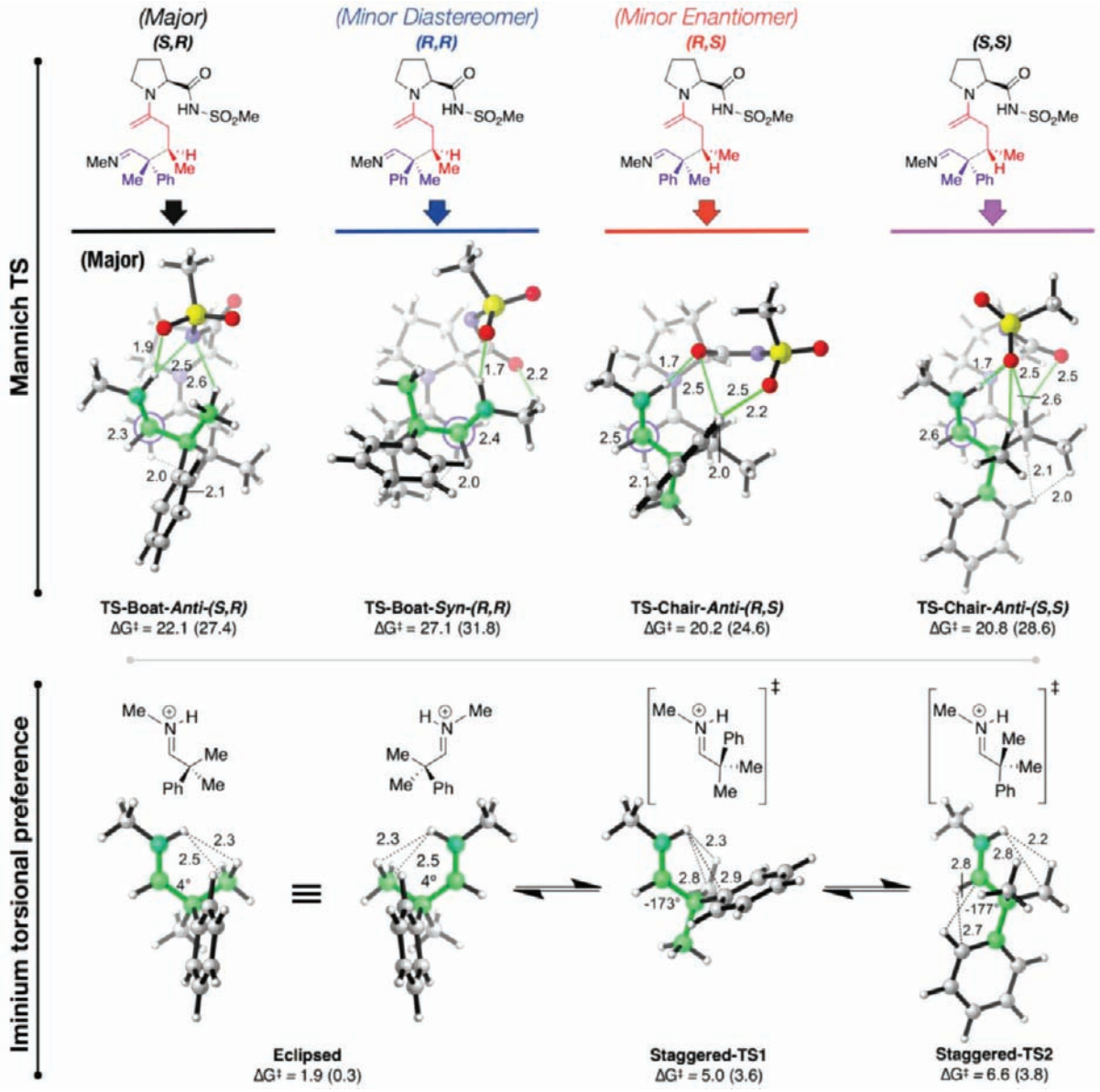

Figure 4. Above: The four Mannich cyclization transition structures consistent with mechanism **A**, leading to the four diastereomeric cyclohexenone products. Boat and chair refer to the conformation of the forming six-membered ring. **TS-Boat-*Syn*-(*R,R*)** determines the diastereoselectivity of this reaction. This transition structure is disfavored compared to the major transition structure **TS-Boat-*Anti*-(*S,R*)** due to severe flagpole interactions stemming from an axial methyl group. Below: Computed conformations of a model acyclic iminium that mimics the transition structures. Analogous atoms are highlighted in green for easy juxtaposition of iminium conformations. The eclipsed iminium conformation found in the twist-boats is more stable than the bisected conformation found in the chairs due to stereoelectronic effects that favor minimizing electrostatic repulsion between the iminium π-system and the α-substituents.[21]

transition structures. This is mainly due to the fact that other stereoisomers are able to adopt stable *anti* conformations in the Mannich annulation transition state. As discussed previously, in general, *anti* transition states are more stable in organocatalytic reactions due to geometric distortions in the planar catalyst iminium that arise in the *syn* transition states. The most well understood example of this effect is found in the proline-catalyzed Mannich and aldol reactions, where this difference in planarity is significant and key to the stereoselectivity.[28] Somewhat unexpectedly, however, there are no significant differences in the planarity of the developing iminium in these Mannich annulation transition structures. Presumably, this is due to the flexibility of the sulfonamide side chain, as well as the unusually wide variation in the length of the forming C−C bonds in these transition structures (2.3−2.9 Å), which distribute the strain over the whole structure.[32] Importantly, there are evident flagpole steric repulsions around the substituents of the forming six-membered ring and the catalyst that dominate the stability of these transition states. For example, the **TS-Boat-*Syn*-(*R,R*)** is conformationally very similar to the **TS-Boat-*Anti*-(*S,R*)**, which leads to the major product. Both are in a twist-boat conformation, and the major hydrogen-bonding interactions are between the sulfonamide and the iminium substituents. However, **TS-Boat-*Syn*-(*R,R*)** is disfavored by 4.4 kcal/mol, because there is a destabilizing steric interaction arising from a methyl group in the axial position of a boat-like forming six-membered ring (2.0 Å steric van der Waals contact, Figure 4). This is in contrast to the

dx.doi.org/10.1021/ja3018219 | J. Am. Chem. Soc. 2012, 134, 13624−13631

epimeric major **TS-Boat-*Syn*-(*S,S*)**, where this same methyl group occupies the equatorial position.

It is interesting to note that the chair and twist-boat Mannich cyclization transition structures are of surprisingly similar stability, with 2.8 kcal/mol separating the most stable chair, **TS-Chair-*Anti*-(*S,S*)**, and the most stable boat, **TS-Boat-*Anti*-(*S,R*)**. This is unexpected, as the chair conformation of cyclohexane is favored over the twist-boat by 5.5 kcal/mol.[33] Two factors contribute to this phenomenon: (a) Chair transition states where multiple substituents are axial are significantly less stable than most boats.[32] (b) Computed conformations of a model acyclic iminium that mimics the transition structures show that the iminium conformation in the twist-boats is more stable than in the chair transition states by >3 kcal/mol (Figure 4, bottom). Specifically, the eclipsed iminium conformation found in the twist-boats is more stable than the bisected conformation found in the chairs due to stereoelectronic effects that favor minimizing electrostatic repulsion between the iminium π-system and the α-substituents.[33] Ultimately, most boat transition structures are still disfavored slightly in comparison to the most stable chairs due to the endemic 1,4-flagpole interactions.

4. CONCLUSIONS

In summary, we have used high-accuracy computational methods to perform an energetically and conformationally exhaustive elucidation of the mechanism and stereocontrol in a dual amino-catalyzed synthesis of cyclohexenones containing all-carbon γ-quaternary and ∂-tertiary stereocenters. Six mechanistic possibilities were considered. We find that the reaction proceeds via a Michael addition between catalyst pentenone iminium and an aldenamine of the α,α-disubstituted aldehyde and the primary amine additive, followed by a Mannich cyclization. An unprecedented duumvirate stereocontrol is present in which the enantioselectivity is set by the first step Michael reaction and the diastereoselectivity by both the Michael and Mannich reactions. In the course of this work, we have identified a combination of theoretical methods that allow for efficient and accurate comparison of transition states across a wide range of mechanisms. The mechanistic and technical discoveries disclosed herein will prove to be of enduring value to other similar efforts in the field. Continuing work in our laboratory focuses on capitalizing on these discoveries toward predictive design and quantitative understanding of new catalytic reactions.

■ ASSOCIATED CONTENT

Supporting Information

Cartesian coordinates and solvation energies. This material is available free of charge via the Internet at http://pubs.acs.org.

■ AUTHOR INFORMATION

Corresponding Author

paulc@science.oregonstate.edu

Notes

The authors declare no competing financial interest.

■ ACKNOWLEDGMENTS

We acknowledge Oregon State University for financial support.

■ REFERENCES

(1) Trost, B. M. *Science* **1991**, *254*, 1471.

(2) Wender, P. A.; Verma, V. A.; Paxton, T. J.; Pillow, T. H. *Acc. Chem. Res.* **2008**, *41*, 40.

(3) (a) Cozzi, P. G.; Hilgraf, R.; Zimmerman, N. *Eur. J. Org. Chem.* **2007**, 5969. (b) Denissova, I.; Barriault, L. *Tetrahedron* **2003**, 10105. (c) Talca, G.; Bella, M. *Synthesis* **2009**, 1583. (d) Marek, I. *Eur. J. Org. Chem.* **2008**, 7460.

(4) (a) Yang, H.; Carter, R. G. *Org. Lett.* **2010**, *12*, 3108. (b) Yang, H.; Carter, R. G. *Synlett* **2010**, *19*, 2827. (c) Cobb, A. J. A.; Shaw, D. M.; Longbottom, D. A.; Gold, J. B.; Ley, S. V. *Org. Biomol. Chem.* **2005**, *3*, 84. (d) Sundén, H.; Dahlin, N.; Ibrahem, I.; Adolfsson, H.; Córdova, A. *Tetrahedron Lett.* **2005**, *46*, 3385.

(5) Becke, A. D. *J. Chem. Phys.* **1993**, *98*, 5648.

(6) (a) Hehre, W. J.; Ditchfield, R.; Pople, J. A. *J. Chem. Phys.* **1972**, *56*, 2257. (b) Hariharan, P. C.; Pople, J. A. *Theor. Chim. Acta* **1973**, *28*, 213.

(7) (a) Dahlke, E. E.; Olson, R. M.; Leverentz, H. R.; Truhlar, D. G. *J. Phys. Chem. A* **2008**, *112*, 3976. (b) Zhao, Y.; Truhlar, D. G. *Theor. Chem. Acc.* **2008**, *120*, 215.

(8) Miertus, S.; Scrocco, E.; Tomasi, J. *J. Chem. Phys.* **1981**, *55*, 117.

(9) Dunning, T. H. *J. Chem. Phys.* **1989**, *90*, 1007.

(10) (a) Grimme, S. *J. Comput. Chem.* **2003**, *24*, 1529. (b) Gerenkamp, M.; Grimme, S. *Chem. Phys. Lett.* **2004**, *392*, 229.

(11) Rapson, W. S.; Robinson, R. *J. Chem. Soc.* **1935**, 1285.

(12) (a) Yang, H.; Carter, R. G. *Org. Lett.* **2008**, *10*, 4649. (b) Yang, H.; Mahapatra, S.; Cheong, P. H.-Y.; Carter, R. G. *J. Org. Chem.* **2010**, *75*, 7279. (c) Enders, D.; Grondal, C.; Vrettou, M.; Gerhard, R. *Angew. Chem., Int. Ed.* **2005**, *44*, 4079. (d) Brogan, A. P.; Dickerson, T. J.; Janda, K. D. *Angew. Chem., Int. Ed.* **2006**, *45*, 8100. (e) Paradowska, J.; Pasternak, M.; Gut, B.; Gryzło, B.; Mlynarski, J. *J. Org. Chem.* **2012**, *77*, 173. (f) Saito, S.; Yamamoto, H. *Acc. Chem. Res.* **2004**, *37*, 570. (g) Cobb, A. J. A.; Shaw, D. M.; Ley, S. V. *Synlett* **2004**, 558.

(13) (a) Unpublished results. (b) Complete consumption of the aldehyde and formation of the imine are observed by ^{1}H NMR when benzylamine and substituted aldehydes are premixed, both with and without molecular sieves.

(14) Huang, X.-Y.; Wang, H.-J.; Shi, J. *J. Phys. Chem. A.* **2010**, *114*, 1068.

(15) (a) Calculations performed with Gaussian 03, 09, and Q-Chem. (b) Frisch, M. J.; Trucks, G. W.; Schlegel, H. B.; Scuseria, G. E.; Robb, M. A.; Cheeseman, J. R.; Scalmani, G.; Barone, V.; Mennucci, B.; Petersson, G. A.; Nakatsuji, H.; Caricato, M.; Li, X.; Hratchian, H. P.; Izmaylov, A. F.; Bloino, J.; Zheng, G.; Sonnenberg, J. L.; Hada, M.; Ehara, M.; Toyota, K.; Fukuda, R.; Hasegawa, J.; Ishida, M.; Nakajima, T.; Honda, Y.; Kitao, O.; Nakai, H.; Vreven, T.; Montgomery, Jr., J. A.; Peralta, J. E.; Ogliaro, F.; Bearpark, M.; Heyd, J. J.; Brothers, E.; Kudin, K. N.; Staroverov, V. N.; Kobayashi, R.; Normand, J.; Raghavachari, K.; Rendell, A.; Burant, J. C.; Iyengar, S. S.; Tomasi, J.; Cossi, M.; Rega, N.; Millam, N. J.; Klene, M.; Knox, J. E.; Cross, J. B.; Bakken, V.; Adamo, C.; Jaramillo, J.; Gomperts, R.; Stratmann, R. E.; Yazyev, O.; Austin, A. J.; Cammi, R.; Pomelli, C.; Ochterski, J. W.; Martin, R. L.; Morokuma, K.; Zakrzewski, V. G.; Voth, G. A.; Salvador, P.; Dannenberg, J. J.; Dapprich, S.; Daniels, A. D.; Farkas, Ö.; Foresman, J. B.; Ortiz, J. V.; Cioslowski, J.; Fox, D. J. *Gaussian 09*, Revision A.1; Gaussian, Inc.: Wallingford, CT, 2009. (c) Frisch, M. J.; Trucks, G. W.; Schlegel, H. B.; Scuseria, G. E.; Robb, M. A.; Cheeseman, J. R.; Montgomery, Jr., J. A.; Vreven, T.; Kudin, K. N.; Burant, J. C.; Millam, J. M.; Iyengar, S. S.; Tomasi, J.; Barone, V.; Mennucci, B.; Cossi, M.; Scalmani, G.; Rega, N.; Petersson, G. A.; Nakatsuji, H.; Hada, M.; Ehara, M.; Toyota, K.; Fukuda, R.; Hasegawa, J.; Ishida, M.; Nakajima, T.; Honda, Y.; Kitao, O.; Nakai, H.; Klene, M.; Li, X.; Knox, J. E.; Hratchian, H. P.; Cross, J. B.; Bakken, V.; Adamo, C.; Jaramillo, J.; Gomperts, R.; Stratmann, R. E.; Yazyev, O.; Austin, A. J.; Cammi, R.; Pomelli, C.; Ochterski, J. W.; Ayala, P. Y.; Morokuma, K.; Voth, G. A.; Salvador, P.; Dannenberg, J. J.; Zakrzewski, V. G.; Dapprich, S.; Daniels, A. D.; Strain, M. C.; Farkas, O.; Malick, D. K.; Rabuck, A. D.; Raghavachari, K.; Foresman, J. B.; Ortiz, J. V.; Cui, Q.; Baboul, A. G.; Clifford, S.; Cioslowski, J.; Stefanov, B. B.; Liu, G.; Liashenko, A.; Piskorz, P.; Komaromi, I.; Martin, R. L.; Fox, D. J.; Keith, T.; Al-Laham, M. A.; Peng, C. Y.;

Nanayakkara, A.; Challacombe, M.; Gill, P. M. W.; Johnson, B.; Chen, W.; Wong, M. W.; Gonzalez, C.; Pople, J. A. *Gaussian 03*, Revision C.02; Gaussian, Inc.: Wallingford, CT, 2004. (d) Shao, Y.; Molnar, L. F.; Jung, Y.; Kussmann, J.; Ochsenfeld, C.; Brown, S. T.; Gilbert, A. T. B.; Slipchenko, L. V.; Levchenko, S. V.; O'Neill, D. P.; DiStasio, R. A., Jr; Lochan, R. C.; Wang, T.; Beran, G. J. O.; Besley, N. A.; Herbert, J. M.; Yeh Lin, C.; Van Voorhis, T.; Hung Chien, S.; Sodt, A.; Steele, R. P.; Rassolov, V. A.; Maslen, P. E.; Korambath, P. P.; Adamson, R. D.; Austin, B.; Baker, J.; Byrd, E. F. C.; Dachsel, H.; Doerksen, R. J.; Dreuw, A.; Dunietz, B. D.; Dutoi, A. D.; Furlani, T. R.; Gwaltney, S. R.; Heyden, A.; Hirata, S.; Hsu, C.-P.; Kedziora, G.; Khalliulin, R. Z.; Klunzinger, P.; Lee, A. M.; Lee, M. S.; Liang, W.; Lotan, I.; Nair, N.; Peters, B.; Proynov, E. I.; Pieniazek, P. A.; Min Rhee, Y.; Ritchie, J.; Rosta, E.; David Sherrill, C.; Simmonett, A. C.; Subotnik, J. E.; Lee Woodcock, H., III; Zhang, W.; Bell, A. T.; Chakraborty, A. K.; Chipman, D. M.; Keil, F. J.; Warshel, A.; Hehre, W. J.; Schaefer, H. F., III; Kong, J.; Krylov, A. I.; Gill, P. M. W.; Head-Gordon, M. *Phys. Chem. Chem. Phys.* **2006**, *8*, 3172.

(16) See Supporting Information for the lowest energy Michael addition and Mannich annulation transition-state structures in mechanism **A** calculated with M06/6-31G*, as well as a comparison of the calculated equilibrium between starting materials and imine formation using B3LYP/6-31G*, M06/6-31G*, and SCS-MP2/∞//B3LYP/6-31G*.

(17) (a) Rokob, T. A.; Hamza, A.; Papai, I. *Org. Lett.* **2007**, *9*, 4279. (b) Wheeler, S. E.; Moran, A.; Pieniazek, S. N.; Houk, K. N. *J. Phys. Chem. A* **2009**, *113*, 10376. (c) Singh, R. K.; Tsuneda, T.; Hirao, K. *Theor. Chem. Acc.* **2011**, *130*, 153.

(18) Another step, such as iminium formation or enamine formation, may be rate limiting, as demonstrated by Meyer and Houk: (a) Zhu, H.; Clemente, F. R.; Houk, K. N.; Meyer, M. P. *J. Am. Chem. Soc.* **2009**, *131*, 1632. (b) Clemente, F. R.; Houk, K. N. *Angew. Chem., Int. Ed.* **2004**, *116*, 5890.

(19) This possibility was originally proposed by Benjamin List. See: List, B.; Muller, S. *Synfacts* **2010**, *8*, 944.

(20) Yamada, S.-I.; Otani, G. *Tetrahedron Lett.* **1969**, 4237.

(21) Lowest energy structures are shown. All transition states are pictured as Newman projections viewed along the forming C−C bond. All energies are from SCS-MP2/∞ single points on B3LYP/6-31G* geometries. Vibrational frequencies and thermal corrections are from B3LYP/6-31G*. Solvation corrections were computed with PCM at B3LYP/6-31+G** with UAKS radii for dichloroethane (DCE). Distances are in angstroms, energies in kcal/mol, and angles in degrees. The first energy is gas phase, and the value in parentheses includes solvation corrections. *S* and *R* refer to the absolute configuration of the expected product. *Anti* refers to the conformation in which the catalyst side chain is opposite to the C−C bond-forming carbon, while *syn* refers to being on the same side. *si* and *re* refer to the enamine face. Green lines are heteroatom−hydrogen distances, and dashed lines are hydrogen−hydrogen and hydrogen−carbon distances. All figures of computed structures generated using CYLview 1.0.387: Legault, C. Y. *CYLview* 1.0.387; Université de Sherbrooke, 2009.

(22) Yang, H.; Carter, R. G. *Tetrahedron* **2010**, *66*, 4854.

(23) (a) Juhl, K.; Jorgensen, K. A. *Angew. Chem., Int. Ed.* **2003**, *42*, 1498. (b) For an example of a dual amine-activated Diels−Alder reaction, see: Ramachary, D. B.; Chowdari, N. S.; Barbas, C. F., III *Tetrahedron. Lett.* **2002**, *43*, 6743. (c) Hong, B.-C.; Dange, N. S.; Ding, C.-F.; Liao, J.-H. *Org. Lett.* **2012**, *14*, 448. (d) Zhou, S.-L.; Li, J.-L.; Dong, L.; Chen, Y.-C. *Org. Lett.* **2011**, *13*, 5874. (e) Liu, Y.; Nappi, M.; Arceo, E.; Vera, S.; Melchiorre, P. *J. Am. Chem. Soc.* **2011**, *133*, 15212. (f) Jia, Z.-J.; Jiang, H.; Li, J.-L.; Gschwend, B.; Li, Q.-Z.; Yin, X.; Grouleff, J.; Chen, Y.-C.; Jørgensen, K. A. *J. Am. Chem. Soc.* **2011**, *133*, 5053. (g) For a hetero-Diels−Alder reaction catalyzed by a chiral sulfonamide, see: Kanemitsu, J.; Asajima, Y.; Shibata, T.; Miyazaki, M.; Nagata, K.; Itoh, T. *Heterocycles* **2011**, *83*, 2525.

(24) (a) Yu, T.-Q.; Fu, Y.; Liu, L.; Guo, Q.-X. *J. Org. Chem.* **2006**, *71*, 6157. (b) Guner, V. A.; Houk, K. N.; Davies, I. W. *J. Org. Chem.* **2004**, *69*, 8024. (c) Evanseck, J. D.; Thomas, B. C., IV; Spellmeyer, D. C.; Houk, K. N. *J. Org. Chem.* **1995**, *60*, 7134.

(25) Few enantioselective organocatalytic electrocyclizations are known, and they typically require large chiral counterions to control the torquoselectivity of ring closure. See: (a) Badia, D.; Vicario, J. L. *Chem. Cat. Chem.* **2010**, *2*, 375. (b) Müller, S.; List, B. *Angew. Chem., Int. Ed.* **2009**, *48*, 9975. (c) Maciver, E. E.; Thompson, S.; Smith, M. D. *Angew. Chem., Int. Ed.* **2009**, *48*, 9979. (d) Rueping, M.; Ieawsuwan, W.; Antonchick, A. P.; Nachtsheim, B. J. *Angew. Chem., Int. Ed.* **2007**, *46*, 2097. (e) Maciver, E. E.; Knipe, P. C.; Cridland, A. P.; Thompson, A. L.; Smith, M. D. *Chem. Sci.* **2012**, *3*, 537. Recently, a removable chiral auxiliary was used to control the absolute stereochemistry of an 8π−6π electrocyclization cascade: (f) Kim, K.; Lauher, J. W.; Parker, K. A. *Org. Lett.* **2012**, *14*, 138.

(26) (a) Seebach, D.; Beck, A. K.; Badine, M.; Limbach, M.; Eschenmoser, A.; Treasurywala, A. M.; Hobbi, R. *Helv. Chim. Acta* **2007**, *90*, 425. (b) Kanzian, T.; Lakhdar, S.; Mayr, H. *Angew. Chem., Int. Ed.* **2010**, *49*, 9526. (c) Sharma, A. K.; Sunoj, R. B. *Angew. Chem., Int. Ed.* **2010**, *49*, 6373.

(27) Both the iminium and oxazolidinone intermediates are much too high in energy to serve as parasitic intermediates that prevent catalyst turnover, as has been suggested of oxazolidinones in analogous proline-catalyzed aldol reactions. See citations in ref 26.

(28) *Anti* transition states are usually favored over *syn*: (a) Bahmanyar, S.; Houk, K. N. *J. Am. Chem. Soc.* **2001**, *123*, 12911. (b) Bahmanyar, S.; Houk, K. N. *Org. Lett.* **2003**, *5*, 1249. (c) Bahmanyar, S.; Houk, K. N.; Martin, H. J.; List, B. *J. Am. Chem. Soc.* **2003**, *125*, 2475. (d) Allemann, C.; Gordillo, R.; Clemente, F. R.; Cheong, P. H.-Y.; Houk, K. N. *Acc. Chem. Res.* **2004**, *37*, 558. (e) Cheong, P. H.-Y.; Houk, K. N. *Synthesis* **2005**, *9*, 1533. (f) Cheong, P. H.-Y.; Zhang, H.; Thayumanavan, R.; Tanaka, F.; Houk, K. N.; Barbas, C. F. *Org. Lett.* **2006**, *8*, 811. (g) Cheong, P. H.-Y.; Legault, C. Y.; Um, J. M.; Çelebi-Olçüm, N.; Houk, K. N. *Chem. Rev.* **2011**, *111*, 5042.

(29) Occasionally *syn* transition states are favored over *anti*: (a) Mitsumori, S.; Zhang, H.; Cheong, P. H.-Y.; Houk, K. N.; Tanaka, F.; Barbas, C. F. *J. Am. Chem. Soc.* **2006**, *128*, 104. (b) Houk, K. N.; Cheong, P. H.-Y. *Nature* **2008**, *455*, 309. (c) Kunz, R. K.; MacMillan, D. W. C. *J. Am. Chem. Soc.* **2005**, *127*, 3240.

(30) (a) Mukherjee, S.; Yang, J. W.; Hoffmann, S.; List, B. *Chem. Rev.* **2007**, *107*, 5471. (b) Patil, M. P.; Sharma, A. K.; Sunoj, R. B. *J. Org. Chem.* **2010**, *75*, 7310. (c) List, B. *Chem. Commun.* **2006**, 819. (d) Erkkilä, A.; Majander, I.; Pihko, P. M. *Chem. Rev.* **2007**, *107*, 5416. (e) Jensen, K. L.; Dickmeiss, G.; Jiang, H.; Albrecht, L.; Jørgensen, K. A. *Acc. Chem. Res.* **2012**, *45*, 248. (f) Shi, Z.-H.; Sheng, H.; Yang, K.-F.; Jiang, J.-X.; Lai, G.-Q.; Lu, Y.; Xu, L.-W. *Eur. J. Org. Chem.* **2011**, 66.

(31) Consistent with our previous conjecture that the optimal iminium planarity is found in the *syn*-iminium Michael transition states, in the absence of hydrogen-bonding requirements, the key iminium dihedral relaxes to 3° in both of the model transition structures, identical in magnitude to what is observed in the most stable Michael transition state, **TS-*Syn-Re*-(*S,R*)**.

(32) See Supporting Information for a more detailed view of the Mannich transition structures.

(33) Anslyn, E. V.; Dougherty, D. A. *Modern Physical Organic Chemistry*, 1st ed.; University Science Books: Mill Valley, CA, 2006.